# Molecular dynamics calculations of $CH_3$ sticking coefficient onto diamond surfaces

Laurent Schwaederlé[1], Pascal Brault[1], Cathy Rond[2], Alix Gicquel[2]

[1]GREMI, UMR7344, CNRS - Université d'Orléans BP6744,

Orléans Cedex 2,France

[2]LSPM, UPR3407 CNRS, Institut Galilée, Université Paris 13,

93430 Villetaneuse, France

Corresponding author: `Pascal.Brault@univ-orleans.fr`

December 18, 2014

**Abstract.** A molecular dynamics model is implemented in a way dedicated to simulate initial conditions close to microwave plasma deposition of thick single crystal diamond films. The sticking coefficient of $CH_3$ radical is obtained for (111) and (100) surface at three gas and substrate temperatures: 1120, 1200 and 1500 K. A low value of $5 \cdot 10^{-4}$ is obtained, which is consistent with experimental findings claiming values less than 0.01 or equating to $8 \cdot 10^{-3}$ at 1120 K.

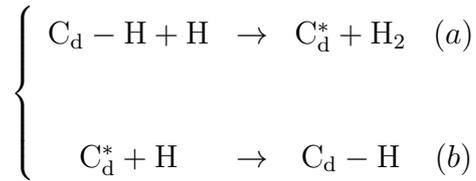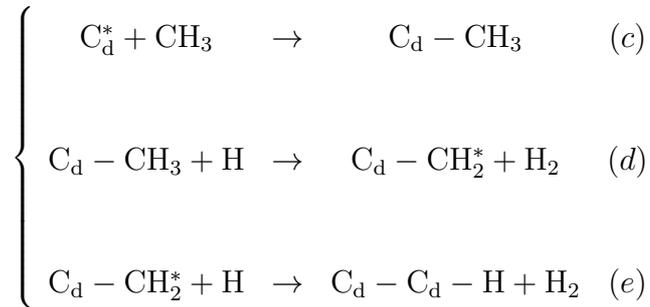**keywords** molecular dynamics; deposition; sticking; diamond; methyl

# 1  Introduction

In power electronics, the semiconductor switching device is a key component because it is a part of all electrical power conversion and control systems [1]. Whereas silicon-based devices still dominate the power electronics applications, Si technology shows difficulty in meeting the demand for some high-power utility applications as a result of limitations in its intrinsic material properties [2]. These limitations as well as the need of weight and volume reduction of power electronics systems require new materials. The wide band gap materials represent the best candidates since they possess better properties than silicon such as breakdown voltage, lower conduction resistance, ... Among them, diamond offers the best combination of properties.

Today, microwave (MW) plasma assisted chemical vapor deposition (MW-PACVD) reactors are the most efficient reactors to produce thick (few 100's $\mu$m) high quality / high purity crystals [3, 4]. However, high power / high pressure conditions are necessary to dissociate efficiently the $H_2$ - (1-10%) $CH_4$ gas mixture. Because of the high gas temperatures reached in the plasma bulk (2800 - 3500 K) [5], the efficient generation of reactive species, in particular atomic hydrogen, a key specie for growing diamond under these conditions, relies on the thermal dissociation of molecular hydrogen rather than on its electron impact dissociation.

Despite several works over the years, the identity of the precursor species for diamond growth is still under discussion. On the one hand, based on either theoretical approach [6, 7, 8, 9, 10] or measurements of the gas com-

position near the substrate [11, 12], it has been suggested that either $C_2H_2$ or $C_2H$ could play a significant role on diamond growth mechanisms. Some molecular dynamics simulations have been carried out in order to reproduce the surface processes for these two species [13, 14]. However, in microwave plasma reactors operating in a moderate pressure range (10 - 300 mbar) and at input microwave powers below 5 kW, methyl radical has been recognized as the main carbon species responsible for diamond growth [15, 5]. On the other hand, Harris and Goodwin have proposed a growth mechanism on the (100) diamond surface, which is the preferred face to growth high quality single crystals [16, 17]. The growth model assumes two main species: the atomic hydrogen H and the methyl radical $CH_3$ that both play key roles. In the model detailed below, the star identifies unsaturated radicals or molecules and Cd means a carbon atom that will be incorporated in the diamond lattice:

$$
\begin{cases}
C_d - H + H & \rightarrow & C_d^* + H_2 \quad (a) \\
\\
C_d^* + H & \rightarrow & C_d - H \quad (b)
\end{cases}
$$

$$
\begin{cases}
\mathrm{C_d^*} + \mathrm{CH_3} & \rightarrow & \mathrm{C_d - CH_3} & (c) \\[2em]
\mathrm{C_d - CH_3} + \mathrm{H} & \rightarrow & \mathrm{C_d - CH_2^*} + \mathrm{H_2} & (d) \\[2em]
\mathrm{C_d - CH_2^*} + \mathrm{H} & \rightarrow & \mathrm{C_d - C_d - H} + \mathrm{H_2} & (e)
\end{cases}
$$

The H atoms 1) stabilize the surface by saturating the dangling bonds, 2) create growth sites, 3) etch the graphitic phase and 4) dehydrogenate the adsorbed radical, while $CH_3$ is the species responsible for diamond film growth. Due to the highly dissociated $H_2$-$CH_4$ plasma, the diamond surface dangling bonds are all saturated by hydrogen atoms giving rise to a surface with sites presenting only $sp^3$ for C-atom configuration. Since the sticking of $CH_3$ on the surface can only take place in a free radical site (dangling bond), the first step must be the creation of radical site that occurs by hydrogen abstraction when hydrogen atoms impact the surface forming $H_2$ molecules that leave the surface (Eley-Rideal mechanism) (a). The most probable fate of this newly created radical site is to be quickly hydrogenated again due to the high atomic hydrogen density and mobility (b). The number of unsaturated dangling bonds on the diamond surface, at any one time, is a function of the equilibrium between these two processes (H abstraction and H addition reactions), which are both sensitive functions of the substrate and gas temperatures. Although the probability is much lower than that of H-atoms, $CH_3$ can react with the surface dangling bonds and stick to them (c). Subsequent dehydrogenation reactions (d) - (e) lead to incorporation of C atoms

into the diamond lattice with a sp$^3$ configuration.

The fraction of dangling bonds (non-hydrogenated surface C atoms) appears to be an important parameter and can be estimated using the relation proposed by May *et al* [18]:

$$R = \frac{1}{1 + 0.3\exp(3430/T_S) + 0.1\exp(-4420/T_s)[H_2]/[H]} \tag{1}$$

where $T_s$ is the surface temperature and $[H_2]$ and $[H]$ the gas-phase densities (in cm$^{-3}$) of molecular and atomic hydrogen in the vicinity of the surface, respectively.

Operating conditions for growing diamond on a (100) face, *i.e.* a substrate temperature of around $T_s$ = 1120 K, a methane percentage in $H_2$-$CH_4$ mixture of 5 % to 7 %, a power higher than 3 kW and a pressure from 200 to 400 hPa [3, 4, 19] give rise to typical densities of $[H_2] = 10^{18}$ cm$^{-3}$ and $[H] = 5 \cdot 10^{15}$ cm$^{-3}$ at the surface [19], it comes a fraction R of 12.5% at $T_s$ = 1120 K, 15% at $T_s$ = 1200 K and 20% at $T_s$ = 1500 K.

In this article, we will assume equilibrium between the two processes (a) and (b) and then a constant fraction of radical site at the surface during simulation in order to analyze the interaction of $CH_3$ radicals with the diamond surface (c).

While molecular dynamics (MD) simulations are well suited for examining basic mechanisms of diamond growth, a rather few ones have been dedicated to gas phase radicals sticking [20, 21, 22, 23, 24, 25, 13, 26, 27, 28, 29, 30].

Among them, Eckert *et al* [22, 23] have simulated the interaction of various radicals, chosen consistently with experimental conditions and findings of May *et al* [31]: incoming radicals are equilibrated at 2120 K prior releasing to the surface, and simulations are performed for substrate temperatures $T_s$ of 800 and 1100 K. $CH_3$ sticking coefficient is shown to be independent of $T_s$ and close to 0.1. However the conditions used in these simulations are relevant for a non-hydrogenated nanodiamond surface and not for hydrogenated single crystalline (100) diamond surface as considered in the present work. A closer work to ours [32] is related to the interaction of various radicals, among them on various surface sites, including hydrogenated sites, but for a-C:H surface not for hydrogenated diamond one. Träskelin *et al* [29, 30] considered interaction with (100) hydrogenated diamond surface and claimed that $CH_3$ sticking coefficient is less than 0.01. But in this case, the diamond surface is maintained at $T_s = 0$ K, which is far from our conditions. Other studies calculate sticking coefficients ranging from 0.1 to 0.6 [24, 25, 28]. But the calculations were carried out using $CH_3$ or C atoms at hyperthermal energies, above 1 eV and rising up to 150 eV. This is also far from the conditions explored here, *i.e.* around 0.1 eV.

The present work is thus intended to determine the $CH_3$ sticking probabilities on (100) and (111) diamond surfaces in conditions consistent with the microwave plasma assisted growth described in ref. [19, 15, 33]. Next section is devoted to the MD procedure consistent with these experimental conditions, while the third section will discuss results for sticking calculation on C(100) and (111) surface at various gas and surface temperature.

6

# 2 The modeling procedure

MD is a computer simulation technique where the time evolution of a set of interacting atoms is followed by integrating the Newton equations of motion. The reactive empirical bond order (REBO) potential from Brenner [34, 35] which is a semi-empirical potential (analytical function for the interaction model whose fitting parameters are chosen in order to reproduce experimental or *ab initio* results) is used. The bond order term which appears in the expression of bond energy modulates the bond strength by the local environment (number of bonds, angle...). Therefore chemical reactions can be accounted for, that is to say this potential can handle bond breaking and formation with appropriate change in hybridization. Solving Newton equations of motion requires the knowledge of the initial positions and velocities of all the atoms of the system. The system is split in two subsystems: the diamond substrate and the $CH_3$ radical. The initial molecular configuration is shown on Fig. 1, where the larger spheres in the lattice represent carbon atoms whereas the smaller spheres at the surface are hydrogen atoms.

Previous studies confirmed that during diamond MW-PACVD growth, the (100) diamond surface is $2 \times 1$ reconstructed and partly hydrogenated, depending on the substrate temperature (see Eq. (1)). We use C(100) $2 \times 1$:H@$x$, $x$=100-R standing for $x$ % of hydrogenated $2 \times 1$ reconstructed (100) diamond surface. The simulated substrate is built using the diamond lattice parameter at the right temperature which is calculated using the relation $\delta a/a = \alpha(T_s)\delta T_s$ where $a$, $T_s$ and $\alpha(T_s)$ are the lattice parameter, the
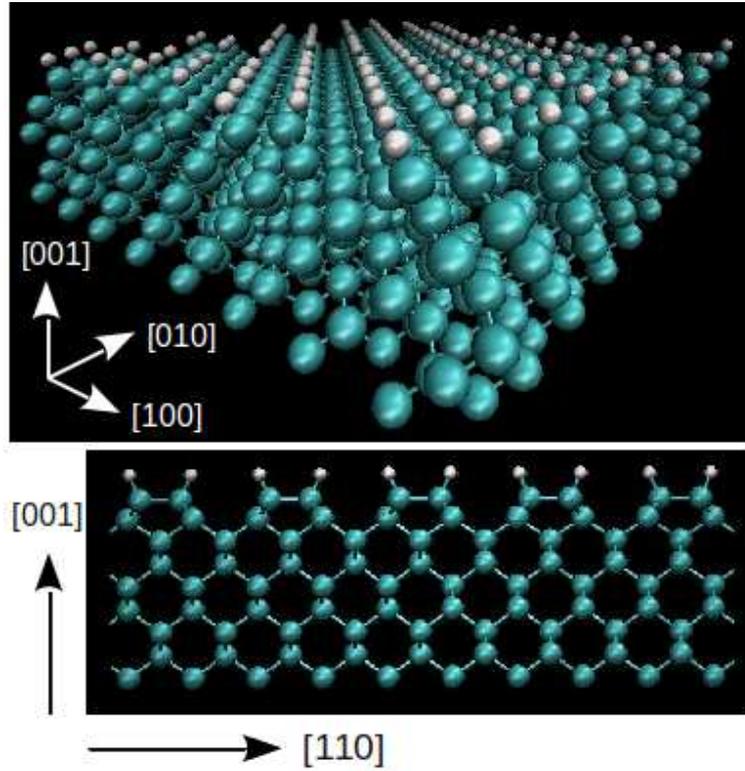
Figure 1: Initial molecular configuration of the diamond substrate

substrate temperature and the isotropic expansion coefficient depending on the substrate temperature respectively. The expansion coefficient $\alpha(T)$ is taken from Ref. [36]. The lattice parameter at $T_s = 1120$ K thus becomes $a_{1120\ K} = 3.5764$ Å, which corresponds to a variation of about 0.3 % with respect to the value at $T_s = 300$ K ($a_{300\ K} = 3.5669$ Å). The value obtained is in good agreement with the one obtained by Gu *et al* [37] using a Local Bond Average model.

The hydrogenated $2 \times 1$ reconstructed surface structure data are taken from Frauenheim *et al* [38] who obtained equilibrium bond length and angles at

8

surface using *ab initio* calculations and which were confirmed by atomic force microscopy observations [39].

The surface radical sites (dangling bonds), created by abstraction reaction of surface H atoms by gas-phase impacting atomic H, can be of two main types [40]: monoradical site (a single dangling bond on a surface carbon) and biradical sites (two surface radical sites on adjacent carbons). Different variants of these mono- and biradical sites exist depending upon the local surface geometry. From Mankelevich *et al* [41], for typical diamond CVD conditions, the fraction of available biradical sites of all types is $\sim 10$ times lower than that of the monoradical sites. We will then assume only monoradical sites at the surface. They are randomly distributed over the surface. The initial configuration of the $CH_3$ radical in the gas phase is shown on Fig. 2. The initial C–H bond length and H–C–H bond angle are taken from Marynick *et al* [42] who reproduced, through *ab initio* calculations, the planar structure of the methyl radical. The initial velocities of all the atoms
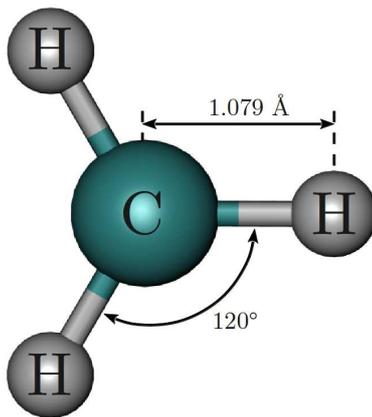


Figure 2: Initial molecular configuration of the methyl radical

9

are randomly sampled from a Maxwell-Boltzmann distribution at the desired gas temperature. The Newton's equations are integrated using the velocity Verlet integration algorithm. For mimicking an infinite system in directions parallel to the substrate, periodic boundary conditions are given in the surface plane directions, corresponding to the [100] and [010] ones for diamond (100) surface. For modeling the thick substrate (bulk material) and to anchor the simulation box, the two lowest carbon atoms layers are kept frozen (static) as shown in Fig. 3. For keeping constant the substrate temperature,
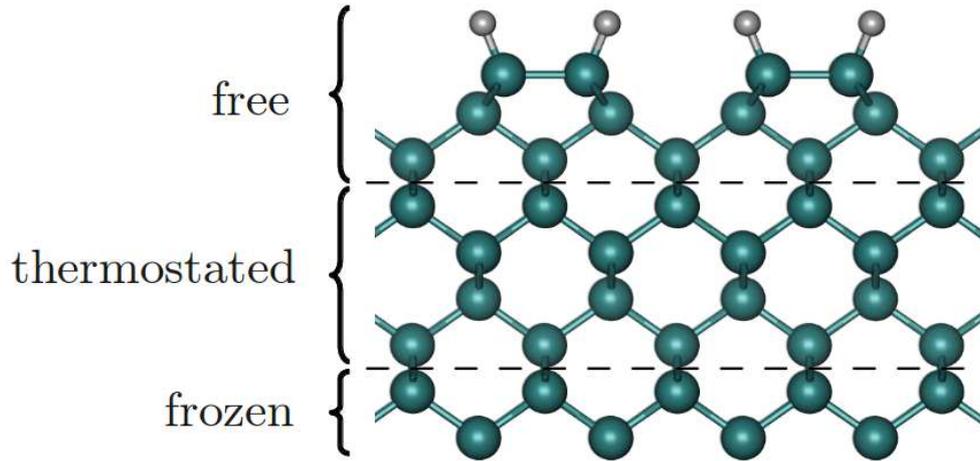


Figure 3: Substrate configuration showing the different atom groups: frozen, thermostated and free

as in the experimental conditions, the four intermediate atoms layers of the substrate model are thermostated using the Berendsen heat bath algorithm [43]. After an equilibrating phase, the model will maintain constant the diamond substrate temperature during the simulation. Carbon and hydrogen atoms in the four upper layers are free to move. All atoms interact through

the REBO potential. We use LAMMPS [1] (Large-scale Atomic/Molecular Massively Parallel Simulator) molecular dynamics solver [44] with a time step of 1 fs.

## 2.1 Equilibration

Before running calculation for the determination of the sticking coefficient of $CH_3$, preliminary molecular dynamics simulation are carried out in order to equilibrate both systems (substrate and radical) at the chosen temperature. The goal of the equilibration phase is not to keep the temperature constant, but rather to ensure that the average temperature of each system be the desired one. The thermalization of the substrate is reached after 5 ps.

The temperature fluctuates around the prescribe experimental value $T_s = 1120$ K. The equilibrated configuration is then stored for the subsequent simulation of the interaction with the incoming $CH_3$ radical. Concerning the methyl radical, to prevent any bias in the calculation of the velocity distribution, the equilibration is carried out for a set of 8000 $CH_3$ radicals using a Nosé -Hoover thermostat chain [45]. Once the equilibrium at the targeted gas temperature is reached, the computation continues for successively storing 8000 radicals to make a list of $CH_3$ configurations which will be used as initial configurations for the subsequent simulation of the interactions with the diamond surface.

Once, the two subsystems are correctly thermalized, they are "merged"

---

[1] http://lammps.sandia.gov

in order to calculate the interaction of the methyl radical with the diamond surface. The sticking coefficient describes the probability of an incoming particle to be trapped in a potential well above a surface. Thus, its determination required a statistical study. Before each elementary calculation, an incident radical is picked up from the previously build $CH_3$ configuration list and is initially placed at a randomly chosen position in the $x$- and $y$-directions and at a distance above the substrate located slightly beyond the potential cutoff distance, where interactions cancel each other out. Only selected radicals having a z-velocity component directed toward the surface are released towards the surface. The calculation time for one interaction is inversely related to the magnitude of the $z$-component of the $CH_3$ velocity, $v_z^{CH_3}$ and thus can be extremely high for the small values of the distribution. To prevent huge calculation time for sampling the whole velocity distribution, we first assume that, due to steric effect, the contribution of the configurations with $v_z^{CH_3} < 100$ m/s is negligible. Present calculations show that no methyl radical with vertical velocity component less than $500$ m.s$^{-1}$ sticks (see discussion below). Secondly, the velocity range is split into intervals $I_v$ of $200$ m.s$^{-1}$ wide. For each such $I_v$ a specific and optimized calculation time is chosen in such a way that each impact is monitored during 1.5 ps.

For each $I_v$ interval, 10 000 elementary interactions are calculated. So with 12 intervals, it means that 120000 impacts are simulated for determining the sticking coefficient SC. $SC_{I_v}$ is the sticking coefficient calculated for each

12

interval as:

$$SC_{I_v} = \frac{\text{number of } CH_3 \text{ with } v_z \in I_v \text{ which sticks}}{\text{total number of incident } CH_3} \qquad (2)$$

Then the global sticking coefficient is obtained by weighting each individual sticking coefficient $SC_{I_v}$ by its corresponding area $A_{I_v}$ under the distribution curve, and summing over all intervals:

$$SC = \sum_{I_v} SC_{I_v} \cdot A_{I_v}. \qquad (3)$$

# 3   Results and discussion

Fig. 4 displays the sticking coefficient for each velocity range at the three different gas and substrate temperatures (1120 K, 1200 K and 1500 K) and for both diamond surfaces, C(100) and C(111). The symbols located on a vertical line represent values of sticking coefficient of $CH_3$ onto both (100) and (111) surfaces, for $CH_3$ having translational kinetic energy normal to the surface within the same range but having different vibrational and rotational energies due to equilibration of the methyl radical vapor at three different gas temperatures. In the gas temperature range explored here, the rotational and vibrational energies thus do not seem to contribute significantly on SC values while only a slight dependence on the gas temperature is observed (except a significant effect at 2500 ms$^{-1}$) as previously observed [23]. The sticking is clearly increasing when increasing kinetic energy, consistently with all previous studies: the sticking coefficient reaches 0.025 on (111) surface and 0.01 on (100) surface. Moreover, at high incoming velocity, the
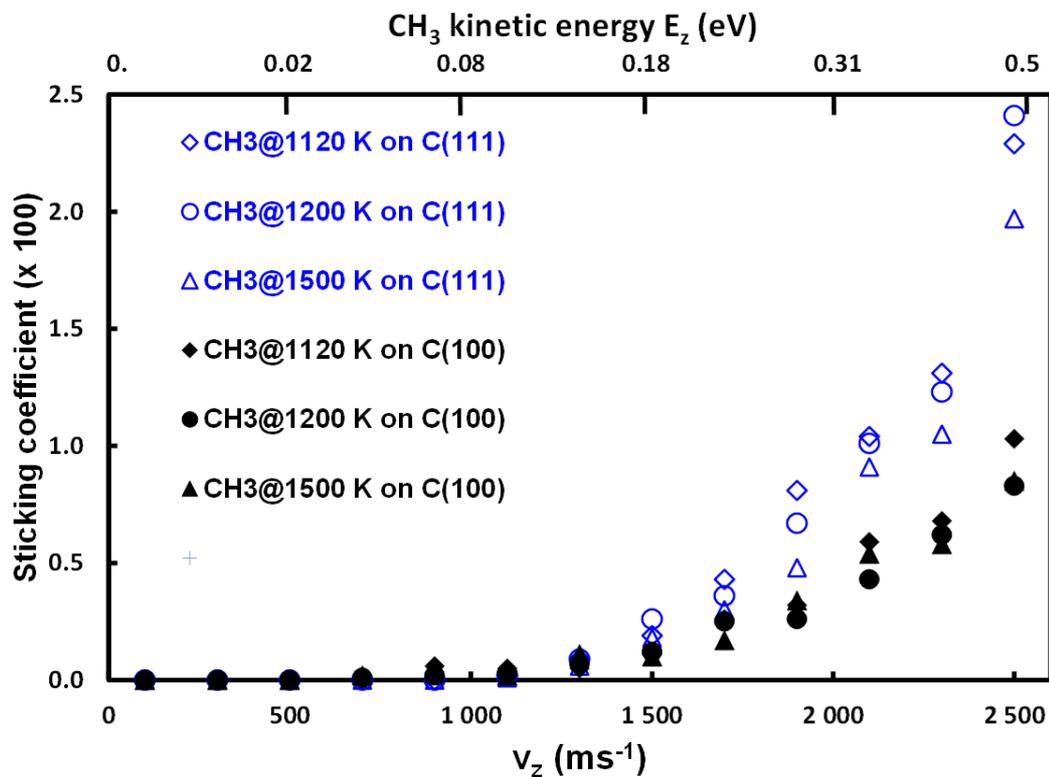
13

Figure 4: Sticking coefficients of $CH_3$ onto diamond surfaces versus the velocity range

(111) surface exhibits a 2 times higher $CH_3$ sticking coefficient (SC =0.025) than for (100) surface. The total sticking coefficients (*i.e.* averaged over the Maxwell-Boltzmann energy distribution of the incoming $CH_3$ radicals) of methyl radical $CH_3$ onto (100) $2 \times 1$:H and (111) $1 \times 1$:H surfaces and their variations with the gas temperature are shown in Fig. 5. Solid line curves represent values obtained for the three different gas temperatures, $T_{CH_3}$=1120, 1200 and 1500 K, with the substrate maintained at constant temperature

$T_s = 1120$ K. The dot line curve is obtained with the substrate and methyl radical vapor in thermal equilibrium at the three temperatures. Thus, the substrate has also been equilibrated at both temperature $T_s = 1200$ K and $T_s = 1500$ K before simulating the interaction with the methyl radical. The
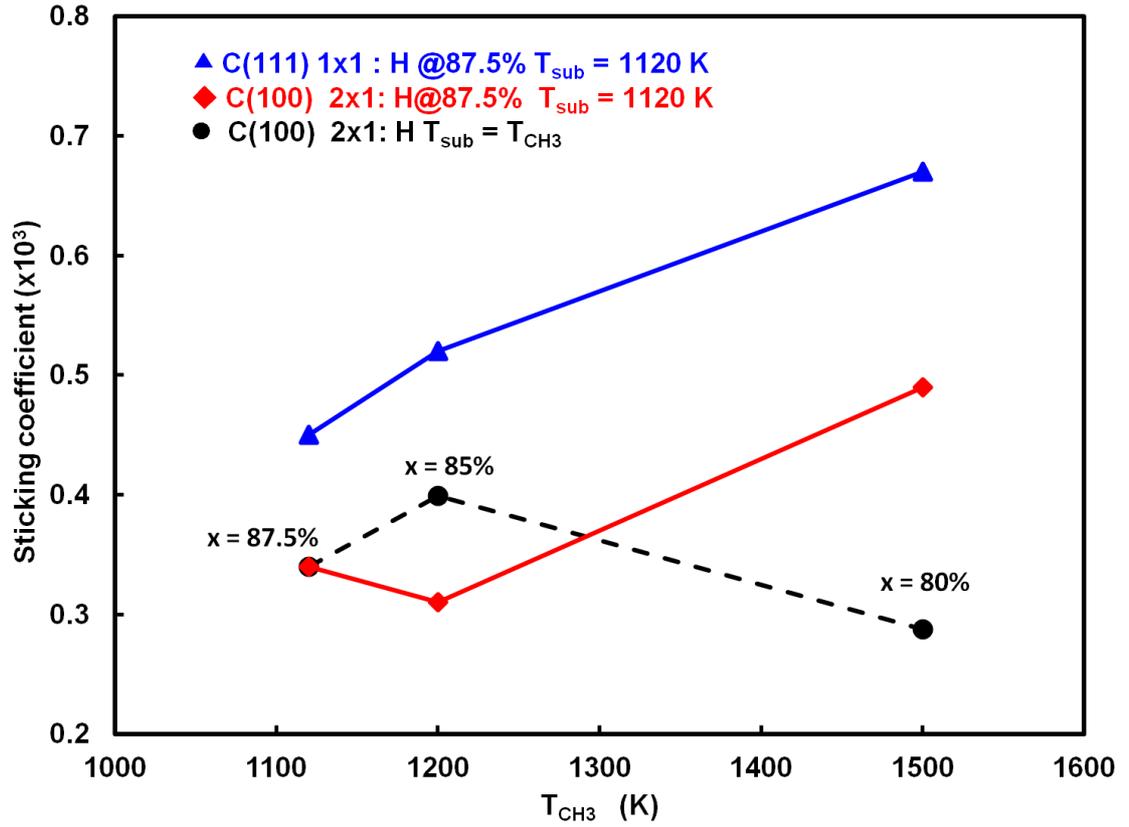


Figure 5: Sticking coefficients of $CH_3$ onto diamond surfaces

total $CH_3$ sticking coefficient is depending on considered surface orientation and on the gas temperature (filled symbols). Moreover, the trend is different when the gas phase is in equilibrium with the substrate: the SC reaches a

maximum equals to $0.4 \cdot 10^{-3}$ at $T_s = T_{CH_3} = 1200$ K before slightly decreasing to $0.28 \cdot 10^{-3}$ at 1500 K. This can be explained by the steric effect enhancement due to the surface temperature increase: while the surface atoms are more vibrating, the probability for reaching and saturating a dangling bond is reduced. Sticking on (111) surface is greater by 30% compared to the (100) one. Furthermore the SC coefficient increases with the gas temperature for (111) surface from $0.45 \cdot 10^{-3}$ to $0.68 \cdot 10^{-3}$ whereas it first decreases before increasing for (100) surface. It has to be compared with the value obtained experimentally by Krasnoperov *et al* [46] who determined the SC by studying the loss of $CH_3$ contained in a discharge flowing over diamond surface by photoionization mass spectrometry. The radicals were produced by laser photolysis of acetone ($[(CH_3)_2CO]$) and the decay of $CH_3$ was time-monitored. They carried out experiments in a heatable flow reactor allowing the determination of the sticking coefficient at a well controlled temperature. They have found a sticking coefficient of about $8 \cdot 10^{-3}$ at 1120 K with an estimated accuracy of $\pm$ 20%. The measured value is one order of magnitude higher than the calculated one. This can be explained by the polycrystalline nature of the diamond surface used in the experiments compared to the perfect (100) and (111) surface used in calculations. The grain boundaries are expected to provide more active area for sticking. Moreover, they showed surface temperature dependence of recombination efficiency of methyl radicals on diamond surface which confirms our calculations. This is also consistent with another previous work leading to SC $<$ 0.01 [27].

# 4    Conclusion

MD simulations were carried out for determining the sticking coefficient of $CH_3$ radical in conditions consistent to MWPACVD growth of thick diamond films. The average sticking coefficient is found to be very low and ranges in $[0.28 - 0.68] \cdot 10^{-3}$ for the studied conditions of temperatures and substrate orientation, which is consistent with experimental findings and some MD results on hydrogenated diamond surface. Both temperature and velocity range dependence of the sticking coefficient evolution are consistent with previous MD calculations whatever the substrate is.

# Acknowledgments

# References

[1] Zhe Chen, J.M. Guerrero, and F. Blaabjerg. A review of the state of the art of power electronics for wind turbines. *IEEE Transactions on Power Electronics*, 24(8):1859–1875, 2009.

[2] J. Achard, F. Silva, R. Issaoui, O. Brinza, A. Tallaire, H. Schneider, K. Isoird, H. Ding, S. Kon, M.A. Pinault, F. Jomard, and A. Gicquel.

Thick boron doped diamond single crystals for high power electronics. *Diamond and Related Materials*, 20(2):145–152, February 2011.

[3] Jocelyn Achard, Alexandre Tallaire, Ricardo Sussmann, Franois Silva, and Alix Gicquel. The control of growth parameters in the synthesis of high-quality single crystalline diamond by CVD. *Journal of Crystal Growth*, 284(34):396–405, November 2005.

[4] J Achard, F Silva, A Tallaire, X Bonnin, G Lombardi, K Hassouni, and A Gicquel. High quality MPACVD diamond single crystal growth: high microwave power density regime. *Journal of Physics D: Applied Physics*, 40(20):6175–6188, October 2007.

[5] K Hassouni, F Silva, and A Gicquel. Modelling of diamond deposition microwave cavity generated plasmas. *Journal of Physics D: Applied Physics*, 43(15):153001, April 2010.

[6] K. Larsson. Nearest-neighbor influence on hydrocarbon adsorption on diamond (111) studied by ab initio calculations. *Physical Review B*, 51(15):10003–10012, 1995.

[7] Michael Frenklach and Karl E. Spear. Growth mechanism of vapor-deposited diamond. *Journal of Materials Research*, 3:133–140, 2 1988.

[8] XiaoYan Chang, Donald L. Thompson, and Lionel M. Raff. Minimum-energy paths for elementary reactions in low-pressure diamond-film formation. *The Journal of Physical Chemistry*, 97(39):10112–10118, 1993.

[9] James Peploski, Donald L. Thompson, and Lionel M. Raff. Molecular dynamics studies of elementary surface reactions of acetylene and ethynyl radical in low-pressure diamond-film formation. *The Journal of Physical Chemistry*, 96(21):8538–8544, 1992.

[10] Hans Rau and Friederike Picht. Modeling of diamond growth from a microwave plasma: C2h as growth species. *Journal of Materials Research*, 8:2250–2264, 9 1993.

[11] Peter Dek, Antal Kovts, Peter Cskvry, Istvn Maros, and Gyrgy Hrs. Ethynyl (c2h): A major player in the chemical vapor deposition of diamond. *Applied Physics Letters*, 90(5):–, 2007.

[12] M. A. Cappelli and P. H. Paul. An investigation of diamond film deposition in a premixed oxyacetylene flame. *Journal of Applied Physics*, 67(5):2596–2602, 1990.

[13] Erik Neyts, A. Bogaerts, R. Gijbels, J. Benedikt, and M.C.M. van de Sanden. Molecular dynamics simulations for the growth of diamond-like carbon films from low kinetic energy species. *Diamond and Related Materials*, 13(10):1873 – 1881, 2004.

[14] P. Trskelin, O. Saresoja, and K. Nordlund. Molecular dynamics simulations of c2, C2H, C2H2, C2H3, C2H4, C2H5, and C2H6 bombardment of diamond (1 1 1) surfaces. *Journal of Nuclear Materials*, 375(2):270–274, April 2008.

[15] G Lombardi, K Hassouni, G D Stancu, L Mechold, J Rpcke, and A Gicquel. Study of an h 2/CH4 moderate pressure microwave plasma used for diamond deposition: modelling and IR tuneable diode laser diagnostic. *Plasma Sources Science and Technology*, 14(3):440–450, August 2005.

[16] D. G. Goodwin. Scaling laws for diamond chemicalvapor deposition. i. diamond surface chemistry. *Journal of Applied Physics*, 74(11):6888–6894, 1993.

[17] D. G. Goodwin. Scaling laws for diamond chemicalvapor deposition. ii. atomic hydrogen transport. *Journal of Applied Physics*, 74(11):6895–6906, 1993.

[18] Paul W. May and Yuri A. Mankelevich. From ultrananocrystalline diamond to single crystal diamond growth in hot filament and microwave plasma-enhanced CVD reactors: a unified model for growth rates and grain sizes. *Journal of Physical Chemistry C*, 112(32):12432–12441, August 2008.

[19] A. Gicquel, N. Derkaoui, C. Rond, F. Benedic, G. Cicala, D. Moneger, and K. Hassouni. Quantitative analysis of diamond deposition reactor efficiency. *Chemical Physics*, 398(0):239 – 247, 2012. Chemical Physics of Low-Temperature Plasmas (in honour of Prof Mario Capitelli).

[20] Dominic Alfonso. Molecular-dynamics simulations of methyl-radical deposition on diamond (100) surfaces. *Physical Review B*, 48(16):12235–12239, 1993.

[21] D A Alman and D N Ruzic. Molecular dynamics simulation of hydrocarbon reflection and dissociation coefficients from fusion-relevant carbon surfaces. *Physica Scripta*, 2004(T111):145, 2004.

[22] Maxie Eckert, Erik Neyts, and Annemie Bogaerts. Molecular dynamics simulations of the sticking and etch behavior of various growth species of (Ultra)Nanocrystalline diamond films. *Chemical Vapor Deposition*, 14(7-8):213–223, 2008.

[23] M Eckert, E Neyts, and A Bogaerts. On the reaction behaviour of hydrocarbon species at diamond (100) and (111) surfaces: a molecular dynamics investigation. *Journal of Physics D: Applied Physics*, 41(3):032006, February 2008.

[24] Z. Huang, Z.Y. Pan, W.J. Zhu, Y.X. Wang, and A.J. Du. Energy dependence of methyl-radical adsorption on diamond (001)-(21) surface. *Surface and Coatings Technology*, 141(2-3):246–251, June 2001.

[25] H.-P. Kaukonen and R. M. Nieminen. Molecular-dynamics simulation of the growth of diamondlike films by energetic carbon-atom beams. *Phys. Rev. Lett.*, 68:620–623, Feb 1992.

[26] E. Neyts and A. Bogaerts. Influence of internal energy and impact angle on the sticking behaviour of reactive radicals in thin a-c:h film growth:

a molecular dynamics study. *Phys. Chem. Chem. Phys.*, 8:2066–2071, 2006.

[27] A. von Keudell, C. Hopf, T. Schwarz-Selinger, and W. Jacob. Surface loss probabilities of hydrocarbon radicals on amorphous hydrogenated carbon film surfaces: Consequences for the formation of re-deposited layers in fusion experiments. *Nuclear Fusion*, 39:1451, 1999.

[28] Klaus Tichmann, Udo von Toussaint, and Wolfgang Jacob. Determination of the sticking coefficient of energetic hydrocarbon molecules by molecular dynamics. *Journal of Nuclear Materials*, 420(13):291 – 296, 2012.

[29] P. Traskelin, E. Salonen, K. Nordlund, A. V. Krasheninnikov, J. Keinonen, and C. H. Wu. Molecular dynamics simulations of CH3 sticking on carbon surfaces. *Journal of Applied Physics*, 93(3):1826, 2003.

[30] P Trskelin, E Salonen, K Nordlund, J Keinonen, and C.H Wu. Molecular dynamics simulations of CH3 sticking on carbon surfaces, angular and energy dependence. *Journal of Nuclear Materials*, 334(1):65–70, August 2004.

[31] Paul W. May. Diamond thin films: a 21st-century material. *Philosophical Transactions of the Royal Society of London. Series A: Mathematical, Physical and Engineering Sciences*, 358(1766):473 –495, January 2000.

[32] E. Neyts, M. Tacq, and A. Bogaerts. Reaction mechanisms of low-kinetic energy hydrocarbon radicals on typical hydrogenated amorphous carbon (a-c:h) sites: A molecular dynamics study. *Diamond and Related Materials*, 15(10):1663 – 1676, 2006.

[33] G Lombardi, G D Stancu, F Hempel, A Gicquel, and J Rpcke. Quantitative detection of methyl radicals in non-equilibrium plasmas: a comparative study. *Plasma Sources Science and Technology*, 13(1):27–38, February 2004.

[34] Donald Brenner. Empirical potential for hydrocarbons for use in simulating the chemical vapor deposition of diamond films. *Physical Review B*, 42(15):9458–9471, 1990.

[35] Donald W Brenner, Olga A Shenderova, Judith A Harrison, Steven J Stuart, Boris Ni, and Susan B Sinnott. A second-generation reactive empirical bond order (REBO) potential energy expression for hydrocarbons. *Journal of Physics: Condensed Matter*, 14(4):783–802, February 2002.

[36] P. Pavone. Ab initio lattice dynamics of diamond. *Physical Review B*, 48(5):3156–3163, 1993.

[37] Mingxia Gu, Yichun Zhou, and Chang Q. Sun. Local bond average for the thermally induced lattice expansion. *The Journal of Physical Chemistry B*, 112(27):7992–7995, July 2008.

[38] Th. Frauenheim. Stability, reconstruction, and electronic properties of diamond (100) and (111) surfaces. *Physical Review B*, 48(24):18189–18202, 1993.

[39] M. Nimmrich. Atomic-resolution imaging of clean and hydrogen-terminated c(100)-(2x1) diamond surfaces using noncontact AFM. *Physical Review B*, 81(20), 2010.

[40] Sergei Skokov, Brian Weiner, and Michael Frenklach. Elementary reaction mechanism for growth of diamond (100) surfaces from methyl radicals. *J. Phys. Chem.*, 98(28):7073–7082, 1994.

[41] Yu. A. Mankelevich and P.W. May. New insights into the mechanism of CVD diamond growth: Single crystal diamond in MW PECVD reactors. *Diamond and Related Materials*, 17(7–10):1021–1028, October 2008.

[42] Dennis S. Marynick and David A. Dixon. Electron affinity of the methyl radical: Structures of CH3 and CH3-. *Proceedings of the National Academy of Sciences*, 74(2):410–413, January 1977.

[43] H. J. C. Berendsen, J. P. M. Postma, W. F. van Gunsteren, A. DiNola, and J. R. Haak. Molecular dynamics with coupling to an external bath. *The Journal of Chemical Physics*, 81(8):3684, 1984.

[44] Steeve Plimpton. Fast parallel algorithms for short-range molecular dynamics. *Journal of Computational Physics*, 117:1–19, 1995.

[45] Glenn J. Martyna, Michael L. Klein, and Mark Tuckerman. Noséhoover chains: The canonical ensemble via continuous dynamics. *Journal of Chemical Physics*, 97:2635–2643, 1992.

[46] Lev N. Krasnoperov, Ilia J. Kalinovski, Hae Nuh Chu, and David Gutman. Heterogeneous reactions of hydrogen atoms and methyl radicals with a diamond surface in the 300-1133 k temperature range. *The Journal of Physical Chemistry*, 97(45):11787–11796, November 1993.

**Table of Contents**

Efficient processing of diamond single crystal deposition by moderate pressure and power microwave plasma requires knowledge of important basic data, among them the sticking coefficients of the main deposition precursors. This work provides molecular dynamics simulations for a rigorous of the methyl radical sticking coefficient on hydrognated diamond single crystal substrate.